


Rapid isotopic analysis of uranium microparticles via SP-ICP-TOF-MS[☆]

Jordan S. Stanberry^{a,1}, Sarah E. Szakas^{a,1}, Hunter B. Andrews^b, Lyndsey Hendriks^{c,2},
Brian W. Ticknor^a, Rachel A. Bergin^d, Shawna K. Tazik^d, Philip Kegler^e, Stefan Neumeier^e,
N. Alex Zirakparvar^a, Daniel R. Dunlap^a, Benjamin T. Manard^{a,*} 

^a Chemical Sciences Division, Oak Ridge National Laboratory, USA

^b Radioisotope Science and Technology Division, Oak Ridge National Laboratory, USA

^c TOFWERK AG, Thun, Switzerland

^d Savannah River National Laboratory, USA

^e Forschungszentrum Jülich GmbH, Germany

ABSTRACT

Inductively coupled plasma – time-of-flight – mass spectrometry (ICP-TOF-MS) was employed for the isotopic analysis of uranium particles of varying ²³⁵U enrichment levels. Here, a single particle (SP)-based introduction scheme was employed such that individual particles, in a suspension, were analyzed. The uranium oxide microparticles were comprised of depleted uranium (DU, ²³⁵U/²³⁸U of 0.0017316(14)), natural uranium (NU, ²³⁵U/²³⁸U of 0.0072614(39)), and low enriched uranium (LEU, ²³⁵U/²³⁸U of 0.051025(15)). The percent relative difference of the SP-ICP-TOF-MS measured isotopic ratios compared to the expected values for the DU, NU, and LEU particle populations were 8.75, 0.12, and 1.23 %, respectively. After characterization, the DU and NU particles were doped within a complex sample matrix (Arizona Test Dust) containing Fe, Ti, Al, and Si particles, among others. Then, the suspension was analyzed via SP-ICP-TOF-MS and the detected particles were classified as DU or NU based on their measured ²³⁵U/²³⁸U ratio. In the same analysis, the matrix particles (i.e., Al, Fe, and Ti) were detected, demonstrating the simultaneous nuclide detection provided by the measurement platform. The presented SP-ICP-TOF-MS methodology for uranium particle characterization proved to be a high throughput method for detecting and isotopically discerning uranium particles with varying enrichment levels, in a complex matrix.

1. Introduction

Since the Treaty on Non-Proliferation of Nuclear Weapons (NPT) was enacted in 1970, the International Atomic Energy Agency (IAEA) has engaged in nuclear safeguarding activities [1]. Such activities originally focused on verifying declared nuclear materials and activities in countries' nuclear energy programs [1]. However, in the 1990s, the IAEA focus broadened to include detection of undeclared nuclear material and activities, primarily through the new tool of environmental sampling [1–5]. Environmental samples are commonly collected during inspections of nuclear facilities by using cotton swipes to collect particulate debris present on surfaces [1]. The analysis of these environmental samples allow the IAEA to verify the correctness of a nuclear facility

declaration by determining the radionuclide compositions of collected particles. After an inspection, environmental samples are sent to the IAEA's Network of Analytical Laboratories (NWAL) for bulk digestion and/or particle analysis targeted at quantifying and isotopically characterizing the presence of uranium (U) and/or plutonium (Pu) [4]. Bulk analysis typically consists of a complete digestion of the sample, followed by laborious and time intensive purifications [6,7], prior to mass spectrometric analysis via thermal ionization mass spectrometry (TIMS) or inductively coupled plasma - mass spectrometry (ICP-MS) [1,8]. While high-precision isotope ratios and low detection limits are obtained from bulk analysis techniques, information on individual particle compositions is lost [8].

Analysis of particles on environmental samples is often conducted by

This article is part of a special issue entitled: Trends in AAS published in Talanta.

[☆] This manuscript has been authored in part by UT-Battelle, LLC, under contract DE-AC05-00OR22725 with the US Department of Energy (DOE). The US government retains and the publisher, by accepting the article for publication, acknowledges that the US government retains a nonexclusive, paid-up, irrevocable, worldwide license to publish or reproduce the published form of this manuscript, or allow others to do so, for US government purposes. DOE will provide public access to these results of federally sponsored research in accordance with the DOE Public Access Plan (<http://energy.gov/downloads/doe-public-access-plan>).

* Corresponding author.

E-mail address: manardbt@ornl.gov (B.T. Manard).

¹ Both authors contributed equally and should be considered first author.

² Current affiliation: Institute of Analytical Chemistry, Faculty of Chemistry, University of Vienna, Vienna, Austria.

<https://doi.org/10.1016/j.talanta.2025.128578>

Received 3 April 2025; Received in revised form 9 July 2025; Accepted 11 July 2025

Available online 12 July 2025

0039-9140/© 2025 The Authors. Published by Elsevier B.V. This is an open access article under the CC BY license (<http://creativecommons.org/licenses/by/4.0/>).

large geometry - secondary ion mass spectrometry (LG-SIMS) or fission track - thermal ionization mass spectrometry (FT-TIMS) [4,8]. LG-SIMS and FT-TIMS can both provide highly accurate isotopic measurements of individual particles, with low uncertainty [3]. LG-SIMS is capable of automated particle measurements, but is prone to hydride spectral interferences and has lower sensitivity than TIMS [8]. FT-TIMS entails locating individual particles (i.e., the fission track method [8]), subsequently extracting them from a surface and individually mounting them on TIMS filaments. Due to the limited throughput, only a small fraction of the total number of particles are typically analyzed [3,8]. The limited sample throughput of the method, combined with high sample load leads to long turnaround times (typically weeks).

Another approach to particle analysis is laser ablation (LA) – ICP-MS. LA-ICP-MS has been widely applied to the analysis of uranium particles on various ICP-MS platforms, including quadrupole (Q) [9], time-of-flight (TOF) [3], and sector field (SF) with single [10], or multi-collector (MC) detection [11–13]. Benefits of using LA-ICP-MS include its sampling speed, resulting in a high-throughput analysis, as well as the ability to couple it with various techniques and detector types. Manard et al., further augmented LA-MC-ICP-MS by simultaneously conducting laser-induced breakdown spectroscopy (LIBS), which enabled the determination of both the uranium isotope ratios with high precision and the ratio of F/U in UO_2F_2 [12].

An alternative, and relatively unexplored technique to determine isotope ratios in uranium particles is single particle (SP)-ICP-MS. SP-ICP-MS leverages the precise introduction of particles from a liquid suspension into the ICP, with fast detection modalities for elemental and isotopic characterization. The capabilities of SP-ICP-MS make it ideal for the analysis of both nano- and microparticles [14]. ICP-TOF-MS is particularly well suited for SP analysis; its ability to simultaneously measure all elements in the mass range 7–275 amu allows for multi-element analysis in each individual particle [15–22]. This technique has inherently high-throughput, with the ability to analyze thousands of discrete entities, within a single sample, in a matter of minutes [15]. Recent years have seen an emergence in studies employing SP-ICP-TOF-MS to determine isotopic ratios within nanoparticles [23–27].

Using SP-ICP-TOF-MS for isotope ratio determinations within particles has been reported to have RSDs as low as approximately 2 %, with precision directly related to the mass amounts of isotopes present [26]. Considerations for this technique include minimum and maximum particle size limits (as the density and size of a particle relate to the signal response in SP-ICP-MS) [28,29], isotope ratio accuracy, and precision. This work is the first use of SP-ICP-TOF-MS for the isotopic analysis of uranium particles. This is important with regards to sampling and analysis methods set out by IAEA, as this analytical technique could be fit for isotope ratio analysis involving nuclear safeguards and forensics measurements. Results presented here indicate that SP-ICP-TOF-MS can be used to isotopically differentiate U-particles with varying levels of ^{235}U enrichment, including natural, depleted, and low-enriched uranium.

2. Material and methods

2.1. Particles

2.1.1. Depleted uranium particles

Depleted ($^{235}\text{U}/^{238}\text{U} < 0.007$) U_3O_8 microparticles [30] were produced by Savannah River National Laboratory (SRNL) using the SRNL designed THERMALLY EVAPORATED SPRAY FOR ENGINEERED UNIFORM PARTICULATE (THESEUS) platform [31,32]. A 2.05 mM feedstock of depleted uranyl oxalate was flowed (3.0 mL h^{-1}) through a Flow-Focusing Monodisperse Aerosol Generator (FMAG, Model 1520, TSI Inc.) at a frequency of 130 kHz and flow focusing pressure of $2.25 \pm 0.05 \text{ psi}$. Filtered air was used as a carrier gas at a flow rate of $10.0 \pm 0.1 \text{ L min}^{-1}$ to remove excess water from the droplets prior to introduction to a

diffusion drier (Model 3062, TSI, Inc.) and inline heater (Thermo Fisher Lindberg Blue M Mini-Mite Tube Furnace equipped with a 1" Inconel 625 tube) to calcine and oxidize particles from uranyl oxalate to U_3O_8 . The particles were then deposited electrostatically onto 1" diameter silicon planchets (UniversityWafer) using an SRNL-designed mini-aerosol contaminant extractor (Mini-ACE) [33]. The particle population size distribution was confirmed via *in situ* measurements of the geometric standard deviation with an Aerodynamic Particle Sizer (APS, Model 3321, TSI, Inc.) before and after collection onto the substrate. SEM-EDS automated particle analysis (TESCAN MIRA 4) showed an average equivalent circular diameter of $0.89 \pm 0.10 \mu\text{m}$. An average particle density of 5.5 g mL^{-1} was estimated through the reconciliation of APS- and SEM-measured size distributions. These samples were received as dry particles loaded on a planchet and will henceforth be referred to as the "DU" particles.

The DU particles used do not have a certified $^{235}\text{U}/^{238}\text{U}$ ratio and so MC-ICP-MS was to determine the accuracy of the ratio obtained via SP-ICP-TOF-MS. DU particles were digested and analyzed via MC-ICP-MS to accurately determine the bulk $^{235}\text{U}/^{238}\text{U}$ ratio. The stock suspension of DU particles was created by submersing the planchet in ethanol and sonicating for 30 s to suspend the particles. For digestion of the particles, 500 μL of the stock suspension was added to a 15 mL polyfluoroalkoxy alkane (PFA) vial (Saville) and heated on a hot plate at 80°C for 1 h to evaporate the ethanol. Next, 1 mL of $8 \text{ mol L}^{-1} \text{HNO}_3$ (OPTIMA grade, Fisher Chemical) was added, the vial was sealed with its threaded cap, and the sample was heated at 110°C overnight, then allowed to cool to room temperature. Following digestion in the $8 \text{ mol L}^{-1} \text{HNO}_3$, the sample was dried down and resuspended in 1 mL of 2 % HNO_3 (which was prepared by dilution of $8 \text{ mol L}^{-1} \text{HNO}_3$ with ASTM type I water). Next, 100 μL of the digestate was diluted to 1 mL using 2 % nitric acid and then analyzed for $^{235}\text{U}/^{238}\text{U}$ ratio using MC-ICP-MS (Neptune Plus, ThermoFisher, Germany).

The Neptune Plus MC-ICP-MS is outfitted with a multiple ion counter package including three secondary electron multipliers (EM), two of which have retarding potential quadrupole filters (RPQ), and two compact discrete diode (CDD) detectors. For the analysis of the digested U particles, ^{238}U was measured on the L4 faraday cup and ^{235}U on the L5 faraday cup, both equipped with $10^{11} \Omega$ resistance amplifiers, while ^{234}U and ^{236}U were measured on EMs equipped with RPQs. This sequence ran triplicate analyses of the digested U particles as well as process blanks, mass bias corrections, and CRMs IRMM-2020 and IRMM-2022 (uranium quality control standards). Instrumental mass fractionation was corrected using a direct comparison to repeated measurements of CRM IRMM-2025. The digested U particles and the quality control standards (IRMM-2020 and -2022) were all run with a matrix matched acid blank immediately preceding the analyses. The IRMM-2025 mass fractionation comparator standard was run after every two samples or quality control standards. The measurements began with a peak center on ^{238}U followed by 15 cycles each with 8 s of integration time. Corrections were made to account for the hydride contribution by monitoring mass 239 ($^{238}\text{UH}^+$).

2.1.2. Natural uranium particles

The second set of particles was provided by Forschungszentrum Jülich (FZJ) and were synthesized from a certified reference material (CRM 129-A; New Brunswick Laboratory Program Office, NBL PO) with natural uranium isotopic composition using an aerosol-based method similar to that of SRNL. The procedure is described in more detail elsewhere [34,35]. A uranyl nitrate solution ($111.8 \mu\text{g U g}^{-1}$) was pumped with a flow rate of $2.6 \mu\text{L s}^{-1}$ into a Vibrating Orifice Aerosol Generator (VOAG 3450, TSI, Inc.) to generate an aerosol jet using a 20 μm orifice (TSI, Inc.) vibrating with a frequency of 70 kHz. The aerosol droplets were dried in a purified air stream (18 L min^{-1}) to form uranyl nitrate particles that were transformed in an aerosol heater (Dekati, Finland) at 500°C to the more stable uranium oxide form. Subsequently, monodisperse microparticles with diameter of $1.2 \mu\text{m}$ were collected on

Table 1
ICP-TOF-MS instrument parameters used when running each sample set.

Instrument Parameter	NU and LEU Particles	DU Particles and Mixture
Nebulizer Gas (Ar L min ⁻¹)	0.54	0.53
Additional Gas (Ar L min ⁻¹)	0.35	0.33
Auxiliary (Ar L min ⁻¹)	0.82	0.82
Cool Gas (Ar L min ⁻¹)	14.01	14.43
Sampling Depth (mm)	6	6
RF Power (W)	1550	1550
CCT Mass (V)	146	167
CCT Bias (V)	3.32	2.22
CCT Gas (He mL min ⁻¹)	5.02	2.40
Notch (m/z (V))	40 (1.5), 30.5 (2), 36(1.5), 241 (1)	40.5 (1.7), 16.3 (2), 30.5 (2), 241 (1)
Acquisition Time	2 ms	2 ms

quartz discs for 1 h. These particles were received as a suspension in ethanol and will henceforth be referred to as the ‘NU’ particles.

2.1.3. Low enriched uranium particles

Uranium particles (IRMM-2331P) were procured as a certified uranium particle reference material [4] from the Joint Research Centre (Geel, Belgium). They have a ²³⁵U/²³⁸U ratio of 0.051025(15) [4] and will be henceforth referred to as the ‘LEU’ particles. The particles were received as dry particles loaded on a planchet. The synthesis of these particles has been described in detail elsewhere [36].

2.1.4. Arizona Test Dust

Arizona Test Dust (ATD, ISO-12103-1), from Powder Technology, was utilized as a sample matrix to demonstrate the multi-isotopic capabilities of SP-ICP-TOF-MS. ATD is composed of particulate SiO₂ (68–76 wt%), Al₂O₃ (10–15 wt%), Fe₂O₃ (2–5 wt%), Na₂O (2–4 wt%), CaO (2–5 wt%), MgO (1–2 wt%), TiO₂ (0.5–1 wt%), and K₂O (2–5 wt%). The ATD particles are <0.3 µm in diameter.

2.2. Preparation of particle suspensions

Stock suspensions of DU and LEU particles were created by

submersing the planchets in ethanol (Supelco, EMSURE®) and sonicating them for 30 s to suspend the particles. The NU sample was received already suspended in ethanol.

The samples containing a single type of uranium particle were prepared by volumetric dilution, with ASTM type I water (18.2 MΩ-cm) as follows: 50 µL of NU stock suspension was diluted to a final volume of 1 mL, 20 µL of suspended DU particles was diluted to a final volume of 500 µL (due to limited sample volume), and 100 µL of LEU stock suspension was diluted to a final volume of 1 mL. Particle number concentrations, or PNCs, were estimated based on the number of particles with detected ²³⁸U and an assumed transport efficiency of 40 % (assumed from previous analyses of standard gold nanoparticles (nanoComposix, San Diego, CA, USA) for all runs). The PNCs were approximated at 2×10^5 , 9×10^4 , and 2×10^4 uranium particles mL⁻¹ for NU, DU and LEU, respectively.

ATD was weighed such that ~0.005 g was suspended in 50 mL of water, sonicated for 30 s, and then diluted by ~4700×. Next, 700 µL of this ATD suspension was mixed with 25 µL of the DU stock suspension and 100 µL of the NU stock suspension, which was then diluted to a final volume of 1 mL to create the mixed particle sample. The ratio of ATD particles to uranium particles was ~6:1, with a uranium particle concentration of $\sim 1.5 \times 10^5$ particles mL⁻¹.

2.2.1. SP-ICP-TOF-MS operating parameters

The analyses of suspensions of nano- and microparticles were all conducted using an icpTOF R (TOFWERK AG, Thun, Switzerland) [16, 17]. Samples were delivered to the ICP-TOF-MS at a rate of 10 µL min⁻¹ by a microFAST SC autosampler (ESI, Omaha, NE, USA). The microFAST SC performs mixing steps on samples, resuspending particles and allowing for unattended analysis of nano- and microparticle samples [16]. A high efficiency sample introduction system, composed of a CytoNeb200 (i.d., 150 µm) nebulizer (ESI, Omaha, NE, USA) and CytoSpray spray chamber (ESI, Omaha, NE, USA), was used for enhanced particle transport efficiency [16].

The ICP-TOF-MS was operated in kinetic energy discrimination (KED) mode using ultra high purity (99.999 %) He (Airgas, Radnor, PA, USA). Further instrument parameters can be found in Table 1.

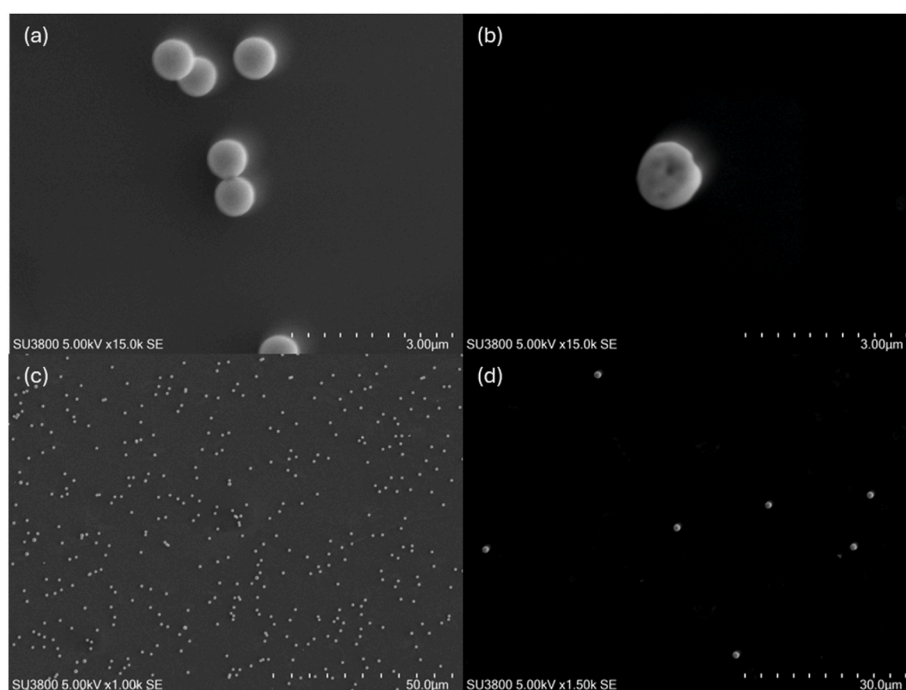


Fig. 1. SEM images of U₃O₈ particles on a silicon wafer. (a) DU particles at 15k zoom, (b) LEU particle at 15k zoom, (c) DU particles at 1k zoom and (d) LEU particles at 1.5k zoom.

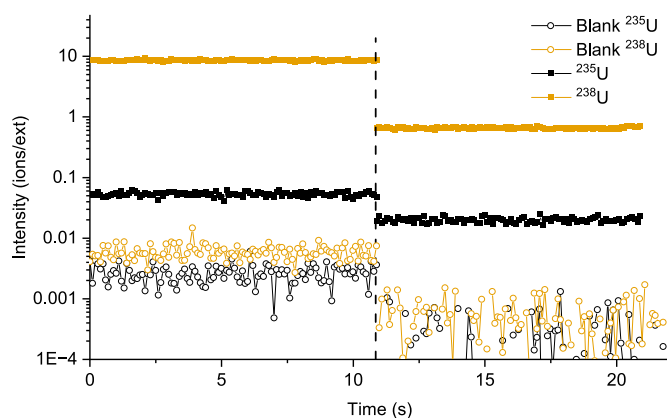


Fig. 2. Measurement of an IRMM-2022 solution, a certified reference material with a $^{235}\text{U}/^{238}\text{U}$ ratio of 0.0072562(12) with different notch filter settings. To the left of the dashed line, no notching was applied. To the right of the line, m/z 241 was notched with an amplitude of 1 V. The line with the empty circles represents the signals recorded in a water blank with both unnotched and notched settings.

3. Results/discussion

3.1. Uranium particle characterization via SEM-EDS

A Hitachi SU3900 scanning electron microscope (SEM) was used to image DU and LEU particles before they were suspended in ethanol (i.e., directly on the planchet). Fig. 1a and b show particle morphology of the DU and LEU, respectively. There are approximately 10^7 particles on the DU wafer, compared to about 10^4 on the LEU wafer; the clear difference in particle number density is shown in Fig. 1c and d. NU particles were not measured via SEM as they were acquired in a suspension.

3.2. ICP-TOF-MS notch filter calibration

SP-ICP-TOF-MS is typically quantitative for elements in the attogram to femtogram range. Here it is being used for the analysis of microparticles in the picogram range (~ 2 – 6 pg of U). The transition from nanoparticles to microparticles represents an increase in mass by a factor of 10^3 to 10^5 , corresponding to a comparable increase in the number of ions per particle. This significant increase in signal intensity can lead to detector saturation, posing a new challenge for accurate measurements. In this approach, He was used as a collision gas to dampen the ion pulse resulting from a single particle, which is needed for these ‘large’ microparticles [37]. However, the use of a collision gas alone is not sufficient signal attenuation for the current application. A feature of the icpTOF R is its notch filter, which is a RF-only quadrupole, allowing it to selectively attenuate high intensity signals, typically from the plasma (N_2^+ , O_2^+ , Ar^+) or sample matrix [17]. Thus, to address detector saturation caused by high ^{238}U -isotope signals, an RF notch filter was used to attenuate the analyte (^{238}U) signal rather than a matrix ion. Shifting the target m/z slightly above ^{238}U allowed reduction of ^{238}U intensity via the filter’s attenuation falloff while minimizing suppression of neighboring ^{235}U . Similar to previous work with Pb isotopes, where notch filters were used to attenuate signals and prevent saturation [38], this

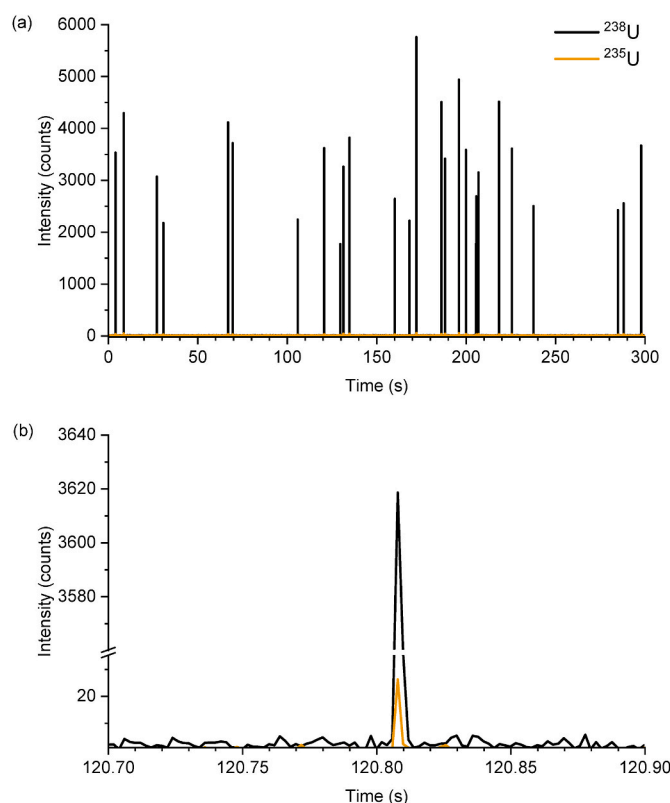


Fig. 3. Time trace of DU particles introduced to SP-ICP-TOF-MS. (a) displays the entire duration of the injection where each signal spike represents a single U_3O_8 particle. (b) Is a zoom in on a single particle detected at 120 s. The break in the y-axis allows a view of the simultaneous detection of both ^{238}U and ^{235}U within the same particle.

approach effectively mitigates signal overload while preserving measurement accuracy. This configuration decreased the ^{238}U signal to ~ 8 % of its original value, while the ^{235}U was only decreased to ~ 37 % of its original value (Fig. 2).

For quantification of $^{235}\text{U}/^{238}\text{U}$ ratios, the selective attenuation of the ^{238}U signal necessitates the determination of a notch calibration factor. These factors were determined via the digested particle suspension, or by aqueous standards (IRMM CRMs), with known $^{235}\text{U}/^{238}\text{U}$ ratios. The notch factor was determined by dividing the known isotopic ratio (via MC-ICP-MS or certified reference value) of the dissolved standard by the average isotope ratio of the standard obtained with the applied notch filter. The particle ratios obtained using the same notch filter were multiplied by this factor to determine their ‘corrected value’. The standards used for each U-particle type and notch correction factors can be found in Table 2. Data collected by SP-ICP-TOF-MS was analyzed using TOF-SPI, incorporating split event correction, and plotted using OriginPro [39].

3.3. Uranium particle analysis by SP-ICP-TOF-MS

Aspiration of a suspension of particles into an ICP-MS at an

Table 2
Summary of notch correction factor.

Analytical Sample	DU	NU	LEU
Standard Used for Notch Corrections	Digested DU	IRMM-2022	IRMM-2029
Expected $^{235}\text{U}/^{238}\text{U}$ Ratio of Standard	0.00173157(24)	0.0072562(12)	0.044052(13)
TOF Notched $^{235}\text{U}/^{238}\text{U}$ Ratio of Standard	0.00317	0.0376	0.178
Notch Correction Factor	0.546	0.193	0.247

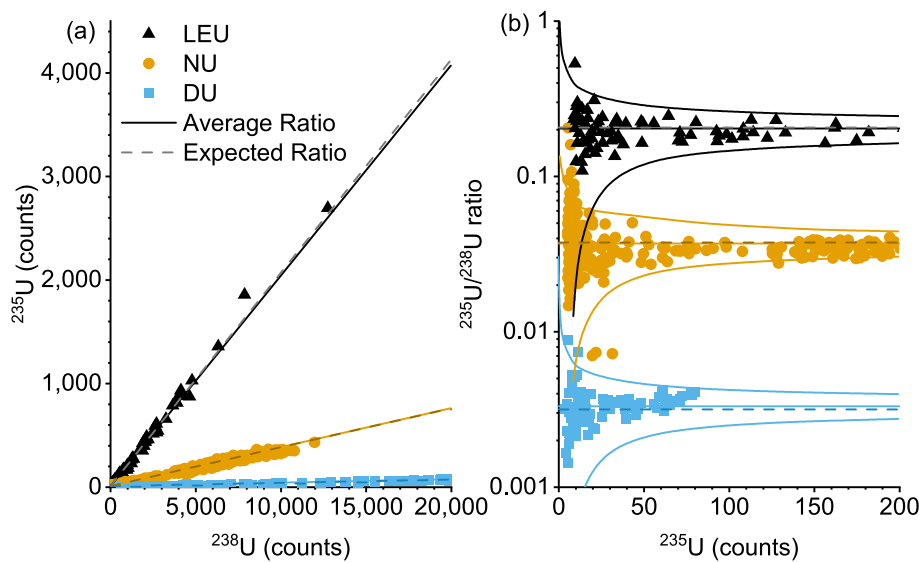


Fig. 4. (a) Counts of ^{235}U vs ^{238}U and (b) $^{235}\text{U}/^{238}\text{U}$ ratio (log scale) as a function of ^{235}U counts from particle suspensions.

Table 3
Summary of measured and expected U-particle isotopic ratios.

Analytical Sample	DU	NU	LEU
Expected $^{235}\text{U}/^{238}\text{U}$ Ratio	0.0017316(14) ^a	0.0072614(39) ^b	0.051025(15) ^c
Average TOF $^{235}\text{U}/^{238}\text{U}$ ratio of sample (uncorrected)	0.00332	0.0376	0.203
Average TOF $^{235}\text{U}/^{238}\text{U}$ ratio of sample (corrected)	0.00189	0.00727	0.0504
Relative difference from expected ratio	8.75 %	0.12 %	1.23 %
Number of particles detected	91	400	107

^a Based on bulk digestion MC-ICP-MS performed in house.
^b Based on certified reference material the particles were synthesized from.
^c The particles themselves are a certified reference material, as detailed in Ref. [4].

appropriate concentration and appropriate dwell/integration times produces a time trace where relatively low background signal is punctuated by high intensity signal spikes, each of which represents a single particle. An example transient, produced by aspirating a suspension of DU particles into the ICP-TOF-MS, is shown in Fig. 3.

Isotope ratios from the SP-ICP-TOF-MS measurements for each sample (DU, NU, and LEU particles) are plotted in Fig. 4. Average ratios were determined using all particles, and are plotted as solid lines in Fig. 4, while the expected ratios, based on the measured particle digest (DU), the certified value of the particle starting material (NU), or certified values of the particles themselves (LEU) - are plotted as dashed lines. Table 3 summarizes the expected isotope ratios of the samples and the ratios measured by SP-ICP-TOF-MS (before and after a notch correction factor was applied). Based on the confidence bands depicted in Fig. 4b, SP-ICP-TOF-MS can reasonably differentiate DU from NU for particles with greater than ~10 counts of ^{235}U . The confidence bands in Fig. 4b are calculated based on Poisson-Normal approximations, with an $\alpha = 0.05$. At least 97 % of each individual particle population is contained within the bounds of these confidence intervals. The intersection of DU's upper confidence interval band and NU's lower confidence interval band occurs at ~10 counts of ^{235}U , which sets a threshold at which these two particle populations are distinguishable based on their isotope ratio. Similarly, at the intersection of NU and LEU confidence interval bands, any U particle type (DU, NU, or LEU) with $^{235}\text{U} > 20$ counts can be differentiated from one another.

Total relative standard deviations (RSDs) surrounding the ratios obtained for DU, NU, and LEU particles were 31 %, 41 %, and 23 %, respectively. These RSDs are reflective of the spread of ratios obtained

within each particle population, and the spread is indicative of the RSD of the measurement itself, which is controlled by Poisson statistics and inherent to the TOF-MS instrument [17,40,41]. Most of the spread in the total RSDs is attributed to particles with low counts of either U isotope (^{238}U or ^{235}U). For example, if only particles with more than 20 counts of ^{235}U are considered, the RSDs within particle populations improve to 11 %, 14 %, and 13 %, respectively.

After using the notch filter to prevent detector saturation, the linear dynamic range (LDR) of the system becomes a critical factor. Harycki and Gundlach-Graham tested the LDR of the icpTOF-S2 (TOFWERK AG) using microdroplets as surrogates for particles, and found that the LDR for individual droplets/particles spanned 1–20,000 counts (per droplet/particle) [42]. Previous studies, which have also reported detector non-linearity due to detector saturation, established a generally accepted cutoff threshold of 20,000 cps [3,40,42,43]. Beyond this range, the detector exhibits non-linear behavior, which can lead to deviations in the measured isotope ratios. The difficulty of measuring these 1 μm particles is partly due to the LDR of the instrument. The depleted uranium measured here nominally has a $^{235}\text{U}/^{238}\text{U}$ ratio of 0.0017316(14), so the expected count rates of ^{235}U and ^{238}U are about three orders of magnitude apart. There is only a narrow count range in which both ^{235}U and ^{238}U counts will be accurately detected. In this work, a non-linear response of the detector was also observed for particles generating >20,000 counts (mostly from ^{238}U). Consequently, all particles exceeding this count threshold were excluded from analysis.

The corrected $^{235}\text{U}/^{238}\text{U}$ ratios for the NU and LEU particles, determined by SP-ICP-TOF-MS, were close to the certificate values; the relative differences were 0.12 % and 1.23 %, respectively. While the LEU

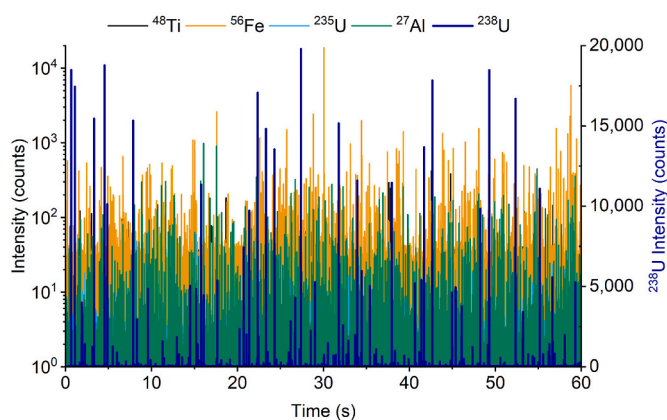


Fig. 5. One minute time trace of sample containing DU, NU, and ATD.

particles should theoretically have the lowest relative difference, it is the NU particles that show the smallest relative difference. This discrepancy may be partially caused by the use of the IRMM-2029 CRM to determine the notch correction factor for LEU particle ratios. IRMM-2029 does not match the expected value of LEU, with a $^{235}\text{U}/^{238}\text{U}$ ratio of 0.044052 (13) (15 % lower than the LEU particles). Due to the non-linear notch effects, it is possible that the notch correction factor obtained from the IRMM-2029 standard is not suitable for the ratios in the LEU particles studied here. Future notch filter studies may better assess how signal is attenuated, but for these samples, or other unknown samples, it would be advisable to run multiple CRMs with samples to best assess which correction factor may need to be employed. The low number of particles detected ($n = 107$) may have also contributed to this higher-than-expected relative difference. The $^{235}\text{U}/^{238}\text{U}$ ratio for the DU particles, as measured by SP-ICP-TOF-MS, had a much larger relative difference of 8.75 %. Both the low ^{235}U count rate for DU particles and low number of particles detected ($n = 91$) contributed to the larger relative difference. The relative difference surrounding the $^{235}\text{U}/^{238}\text{U}$ ratio within particles (Fig. 4) shows that these particle populations can still be differentiated from each other with the measured discrepancy of each isotopic ratio from the certificate value.

The use of various dissolved $^{235}\text{U}/^{238}\text{U}$ standards would allow for accurate correction of notching and determination of $^{235}\text{U}/^{238}\text{U}$ ratios and may mitigate the relative difference discrepancy shown here. For

screening samples, a single standard with known ^{235}U enrichment could even be used to determine if samples are above or below that particular level of ^{235}U enrichment.

3.4. Particle analysis in high matrix

Environmental samples are expected to have dirt, debris, and other particulate matrix inclusions. A suitable analysis technique must therefore be able to accurately determine uranium isotope ratios in a high-matrix sample. An artificial high-matrix sample was created in which DU, NU, and Arizona Test Dust particles were suspended in the same solution. DU and NU were chosen because their isotope ratios are the closest between the three particle types, making them more difficult to differentiate in a mixture. This experiment was carried out to determine if the DU and NU particle populations could still be accurately identified. The SP-ICP-TOF-MS time trace for this mixture is shown in Fig. 5. The multi-element fingerprinting allows for easy differentiation of matrix particles (Fe, Ti, Al) from sample particles (U). Other particles, containing Na, Mg, and Si, were also detected (originating from the ATD), but are not reported here due to their inherently high dissolved backgrounds and low sensitivities.

The $^{235}\text{U}/^{238}\text{U}$ ratio from the spiked NU and DU particles detected in this sample are displayed in Fig. 6. Prior to analyzing the mixed particle sample, the average $^{235}\text{U}/^{238}\text{U}$ ratios and confidence bands (presented in Fig. 6) were determined by running individual suspensions of DU or NU particles under the same experimental conditions as the mixture sample, since tuning and notching parameters affect the absolute sensitivity and isotope ratios. The analysis of individual DU and NU particles was necessary to determine Poisson-Normal confidence bands for mixture data (rather than just using one certified value), as the standard deviation in a particle's ratio is dependent on the counts of each isotope within the particle itself. In these experiments, the average $^{235}\text{U}/^{238}\text{U}$ ratios for DU and NU (uncorrected) were 0.00332 and 0.01233, respectively. By determining the intersection of the confidence bands between particle types, U-particles are again able to be differentiated when they have >23 counts of ^{235}U . At 23 counts of ^{235}U , a threshold $^{235}\text{U}/^{238}\text{U}$ ratio can also be set. This threshold $^{235}\text{U}/^{238}\text{U}$ ratio was determined to be 0.00510; particles below this ratio (and over 23 counts of ^{235}U) were classified as DU and particles above this ratio (and over 23 counts of ^{235}U) were classified as NU.

Approximately equal numbers of DU and NU particles were added to this sample (based on dilutions from the individual particle runs). In

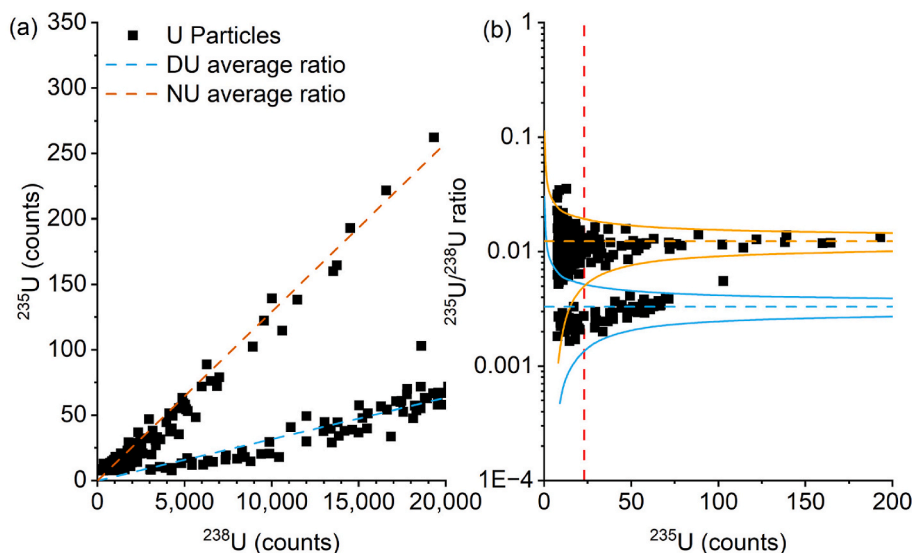


Fig. 6. For the mixed DU and NU sample in ATD. (a) Shows an isotopic plot (^{235}U vs ^{238}U) as a function of counts for ICP-TOF-MS and (b) shows the $^{235}\text{U}/^{238}\text{U}$ ratio as a function of ^{235}U counts. The dashed red line is the ^{235}U counts above which DU and NU can be classified.

total, over 700 U-particles were detected by SP-ICP-TOF-MS. Of these, 316 had detectable amounts of ^{235}U . Using the count/ratio thresholding criteria, 95 (30.1 %) of those particles were classified as DU or NU; 41 were classified as DU and 54 were classified as NU. More particles may have been characterized with different thresholding methods, or efforts to minimize background counts, but setting the count/ratio threshold was fit-for-purpose. Not only were these U-particles classifiable when mixed, but they were also identified in the presence of 1077 Al particles, 655 Fe particles, 293 Ti particles, and >2000 other multi-element particle types (FeAl, FeTi, etc.).

4. Conclusions

Here, SP-ICP-TOF-MS was employed to characterize uranium particles (1 μm) based on their $^{235}\text{U}/^{238}\text{U}$ isotopic ratio. The method enabled the determination of the $^{235}\text{U}/^{238}\text{U}$ ratio in populations of DU, NU, and LEU particles with relative percent differences all below 10 %. Furthermore, the sensitivity of SP-ICP-TOF-MS was enough to obtain accurate ratios, even when DU particles averaged only 26.6 counts of ^{235}U , and had expected ratios ~ 30 times lower than the LEU.

Additionally, SP-ICP-TOF-MS rapidly detected and characterized U-particles as either DU or NU in a complex matrix. Of the 316 classifiable uranium particles, 30.1 % were classified as either DU or NU based on their $^{235}\text{U}/^{238}\text{U}$ ratios. Considering that DU and NU both have a low ^{235}U content and are relatively close in their $^{235}\text{U}/^{238}\text{U}$ ratio, differentiating LEU or higher enrichment level particles from DU or NU is expected to result in a higher percentage of characterizable particles. This unique capability, along with its high-throughput, makes SP-ICP-TOF-MS a promising tool for environmental samples, and could alleviate the analytical burden on more time consuming, laborious, and expensive methods currently utilized, such as FT-TIMS and LG-SIMS.

CRedit authorship contribution statement

Jordan S. Stanberry: Writing – review & editing, Writing – original draft, Methodology, Formal analysis. **Sarah E. Szakas:** Writing – review & editing, Writing – original draft, Investigation, Formal analysis. **Hunter B. Andrews:** Writing – review & editing, Visualization, Formal analysis. **Lyndsey Hendriks:** Writing – review & editing, Software, Formal analysis. **Brian W. Ticknor:** Writing – review & editing, Supervision. **Rachel A. Bergin:** Writing – review & editing, Investigation, Formal analysis. **Shawna K. Tazik:** Writing – review & editing, Funding acquisition, Formal analysis. **Philip Kegler:** Writing – review & editing, Resources, Formal analysis. **Stefan Neumeier:** Writing – review & editing, Resources, Formal analysis. **N. Alex Zirakparvar:** Writing – review & editing, Validation, Formal analysis. **Daniel R. Dunlap:** Writing – review & editing, Validation, Formal analysis. **Benjamin T. Manard:** Writing – review & editing, Visualization, Supervision, Funding acquisition, Formal analysis.

Declaration of competing interest

The authors declare that they have no known competing financial interests or personal relationships that could have appeared to influence the work reported in this paper.

Acknowledgements

This work was supported by the Oak Ridge National Laboratory, managed by UT-Battelle for the Department of Energy under contract DE-AC05-00OR22725. This work was funded by the United States National Nuclear Security Administration's (NNSA) Office of Defense Nuclear Nonproliferation Research & Development. The authors would like to acknowledge Jacquelyn DeMink (ORNL) for assistance with graphics.

Parts of this work were prepared as an account of work sponsored by the Government of the Federal Republic of Germany within the Joint

Programme on the Technical Development and Further Improvement of IAEA Safeguards between the Federal Republic of Germany and the IAEA.

Data availability

Data will be made available on request.

References

- [1] D.L. Donohue, Strengthening IAEA safeguards through environmental sampling and analysis, *J. Alloys Compd.* 271–273 (1998) 11–18.
- [2] V.C. Bradley, J. Burleson, H.B. Andrews, C.V. Thompson, T.L. Spano, D.R. Dunlap, N.A. Zirakparvar, B.W. Ticknor, C.R. Hexel, B.T. Manard, Mapping of uranium particles on J-type swipes with microextraction-ICP-MS, *Analyst* 149 (8) (2024) 2244–2251.
- [3] A.-L. Ronzani, F. Pointurier, M. Rittner, O. Borovinskaya, M. Tanner, A. Hubert, A.-C. Humbert, J. Aupiais, N. Dacheux, Capabilities of laser ablation – ICP-TOF-MS coupling for isotopic analysis of individual uranium micrometric particles, *J. Anal. Atomic Spectrom.* 33 (11) (2018) 1892–1902.
- [4] S. Richter, J. Truyens, C. Venchiarutti, Y. Aregbe, R. Middendorp, S. Neumeier, P. Kegler, M. Klinkenberg, M. Zoriy, G. Stadelmann, Z. Macsik, A. Koepf, M. Sturm, S. Konegger-Kappel, A. Venzin, L. Sangely, T. Tanpraphan, Certification of the first uranium oxide micro-particle reference materials for nuclear safety and security, *IRMM-2329P and IRMM-2331P*, *J. Radioanal. Nucl. Chem.* 332 (7) (2023) 2809–2813.
- [5] G. Tamborini, M. Betti, Characterisation of radioactive particles by SIMS, *Microchim. Acta* 132 (2) (2000) 411–417.
- [6] S.C. Metzger, K.T. Rogers, D.A. Bostick, E.H. McBay, B.W. Ticknor, B.T. Manard, C.R. Hexel, Optimization of uranium and plutonium separations using TEVA and UTEVA cartridges for MC-ICP-MS analysis of environmental swipe samples, *Talanta* 198 (2019) 257–262.
- [7] C.R. Armstrong, B.W. Ticknor, G. Hall, J.R. Cadieux, Rapid separation and purification of uranium and plutonium from dilute-matrix samples, *J. Radioanal. Nucl. Chem.* 300 (2) (2014) 859–866.
- [8] S. Boulyga, S. Konegger-Kappel, S. Richter, L. Sangely, Mass spectrometric analysis for nuclear safeguards, *J. Anal. Atomic Spectrom.* 30 (7) (2015) 1469–1489.
- [9] F. Pointurier, A. Hubert, A.-C. Pottin, Performance of laser ablation: quadrupole-based ICP-MS coupling for the analysis of single micrometric uranium particles, *J. Radioanal. Nucl. Chem.* 296 (2) (2013) 609–616.
- [10] A. Donard, F. Pointurier, A.-C. Pottin, A. Hubert, C. Péchevray, Determination of the isotopic composition of micrometric uranium particles by UV femtosecond laser ablation coupled with sector-field single-collector ICP-MS, *J. Anal. Atomic Spectrom.* 32 (1) (2017) 96–106.
- [11] J. Wimpenny, K.M. Samperton, P. Sotorrio, M.S. Wellons, S.M. Scott, D. Willingham, K. Knight, Rapid isotopic analysis of uranium particles by laser ablation MC-ICP-MS, *J. Anal. Atomic Spectrom.* 38 (4) (2023) 827–840.
- [12] B.T. Manard, C.D. Quarles Jr., V.C. Bradley, T.L. Spano, N.A. Zirakparvar, B.W. Ticknor, D.R. Dunlap, P. Cable-Dunlap, C.R. Hexel, H.B. Andrews, Uranium single particle analysis for simultaneous fluorine and uranium isotopic determinations via laser-induced breakdown spectroscopy/laser ablation-multicollector-inductively coupled plasma-mass spectrometry, *J. Am. Chem. Soc.* 146 (21) (2024) 14856–14863.
- [13] S. Kappel, S.F. Boulyga, T. Prohaska, Direct uranium isotope ratio analysis of single micrometer-sized glass particles, *J. Environ. Radioact.* 113 (2012) 8–15.
- [14] M.D. Montano, J.W. Olesik, A.G. Barber, K. Challis, J.F. Ranville, Single particle ICP-MS: advances toward routine analysis of nanomaterials, *Anal. Bioanal. Chem.* 408 (19) (2016) 5053–5074.
- [15] V.C. Bradley, B.T. Manard, L. Hendriks, D.R. Dunlap, A.N. Bible, A. Sedova, P. Saint-Vincent, B.C. Sanders, H.B. Andrews, Quantifying platinum binding on protein-functionalized magnetic microparticles using single particle-ICP-TOF-MS, *Anal. Methods* 16 (20) (2024) 3192–3201.
- [16] B.T. Manard, V.C. Bradley, C.D. Quarles, L. Hendriks, D.R. Dunlap, C.R. Hexel, P. Sullivan, H.B. Andrews, Towards automated and high-throughput quantitative sizing and isotopic analysis of nanoparticles via single Particle-ICP-TOF-MS, *Nanomaterials* 13 (8) (2023) 1322.
- [17] L. Hendriks, A. Gundlach-Graham, B. Hattendorf, D. Günther, Characterization of a new ICP-TOFMS instrument with continuous and discrete introduction of solutions, *J. Anal. Atomic Spectrom.* 32 (3) (2017) 548–561.
- [18] O. Borovinskaya, S. Gschwind, B. Hattendorf, M. Tanner, D. Günther, Simultaneous mass quantification of nanoparticles of different composition in a mixture by microdroplet Generator-ICP-TOFMS, *Anal. Chem.* 86 (16) (2014) 8142–8148.
- [19] A. Praetorius, A. Gundlach-Graham, E. Goldberg, W. Fabienke, J. Navratilova, A. Gondikas, R. Kaegi, D. Günther, T. Hofmann, F. von der Kammer, Single-particle multi-element fingerprinting (spMEF) using inductively-coupled plasma time-of-flight mass spectrometry (ICP-TOFMS) to identify engineered nanoparticles against the elevated natural background in soils, *Environ. Sci. Nano* 4 (2) (2017) 307–314.
- [20] S. Naasz, S. Weigel, O. Borovinskaya, A. Serva, C. Cascio, A.K. Undas, F.C. Simeone, H.J.P. Marvin, R.J.B. Peters, Multi-element analysis of single nanoparticles by ICP-MS using quadrupole and time-of-flight technologies, *J. Anal. Atomic Spectrom.* 33 (5) (2018) 835–845.
- [21] A. Gondikas, F. von der Kammer, R. Kaegi, O. Borovinskaya, E. Neubauer, J. Navratilova, A. Praetorius, G. Cornelis, T. Hofmann, Where is the nano?

- Analytical approaches for the detection and quantification of TiO₂ engineered nanoparticles in surface waters, *Environ. Sci. Nano* 5 (2) (2018) 313–326.
- [22] H. Karkee, C. Kyte, A. Gundlach-Graham, Classification of zirconium-rich engineered and natural nano particles using single particle ICP-TOFMS, *J. Anal. Atomic Spectrom.* 39 (6) (2024) 1551–1559.
- [23] L. Hendriks, R. Brünjes, S. Taskula, J. Kocić, B. Hattendorf, G. Bland, G. Lowry, E. Bolea-Fernandez, F. Vanhaecke, J. Wang, M. Baalousha, M. von der Au, B. Meermann, T.R. Holbrook, S. Wagner, S. Harycki, A. Gundlach-Graham, F. von der Kammer, Results of an interlaboratory comparison for characterization of Pt nanoparticles using single-particle ICP-TOFMS, *Nanoscale* 15 (26) (2023) 11268–11279.
- [24] G.D. Bland, P. Zhang, E. Valsami-Jones, G.V. Lowry, Application of isotopically labeled engineered nanomaterials for detection and quantification in soils via single-particle inductively coupled plasma time-of-flight mass spectrometry, *Environ. Sci. Technol.* 56 (22) (2022) 15584–15593.
- [25] X. Tian, H. Jiang, M. Wang, W. Cui, Y. Guo, L. Zheng, L. Hu, G. Qu, Y. Yin, Y. Cai, G. Jiang, Exploring the performance of quadrupole, time-of-flight, and multi-collector ICP-MS for dual-isotope detection on single nanoparticles and cells, *Anal. Chim. Acta* 1240 (2023) 340756.
- [26] S.E. Szakas, A. Gundlach-Graham, Isotopic ratio analysis of individual sub-micron particles via spICP-TOFMS, *J. Anal. Atomic Spectrom.* 39 (7) (2024) 1874–1884.
- [27] B.T. Manard, V.C. Bradley, L. Hendriks, D.R. Dunlap, N.A. Zirakparvar, B. W. Ticknor, M. Toro-Gonzalez, H.B. Andrews, Isotopic analysis of Nd nanoparticles using single particle MC-ICP-MS: a comparative study with single particle-ICP-TOF-MS, *Talanta* 286 (2025) 127516.
- [28] J.W. Olesik, P.J. Gray, Considerations for measurement of individual nanoparticles or microparticles by ICP-MS: determination of the number of particles and the analyte mass in each particle, *J. Anal. Atomic Spectrom.* 27 (7) (2012) 1143–1155.
- [29] W.-W. Lee, W.-T. Chan, Calibration of single-particle inductively coupled plasma-mass spectrometry (SP-ICP-MS), *J. Anal. Atomic Spectrom.* 30 (6) (2015) 1245–1254.
- [30] S. Scott, B. Naes, J. Christian, B. Foley, T. Tenner, W. Kuhne, K. Wurth, T. Shehee, S. Lawson, H. Ajo, New particle working standards for NWAL particle laboratory calibration and quality control-operational engineering for an aerosol-based production platform for the synthesis of plutonium-containing reference particulate materials, *Proc. INMM & ESARDA-Joint Annual Meet.* (2023) 22–26.
- [31] B.E. Naes, S. Scott, A. Waldron, S. Lawson, M.G. Bronikowski, L.I. Gleaton, R. J. Smith, K.N. Wurth, T.J. Tenner, M. Wellons, Production of mixed element actinide reference particulates to support nuclear safeguards using THESEUS, an aerosol-based particulate synthetic methodology, *Analyst* 148 (14) (2023) 3226–3238.
- [32] S.M. Scott, A.T. Baldwin, M.G. Bronikowski, M. II, L.A. Inabinet, W.W. Kuhne, B. E. Naes, R.J. Smith, E. Villa-Aleman, T.J. Tenner, Scale-up and production of uranium-bearing QC reference particulates by an aerosol synthesis method. Proceedings of the Joint INMM & ESARDA 2021 Meeting, 2021.
- [33] D.C. Carlson, J.J. DeGange, P. Cable-Dunlap, Portable Aerosol Contaminant Extractor, Savannah River Site (SRS), Aiken, SC (United States), 2005.
- [34] S. Neumeier, R. Middendorp, A. Knott, M. Dürr, M. Klinkenberg, F. Pointurier, D. F. Sanchez, V.-A. Samson, D. Grolimund, I. Niemeyer, Microparticle production as reference materials for particle analysis methods in safeguards, *MRS Advan.* 3 (19) (2018) 1005–1012.
- [35] P. Kegler, F. Pointurier, J. Rothe, K. Dardenne, T. Vitova, A. Beck, S. Hammerich, S. Potts, A.-L. Faure, M. Klinkenberg, F. Kreft, I. Niemeyer, D. Bosbach, S. Neumeier, Chemical and structural investigations on uranium oxide-based microparticles as reference materials for analytical measurements, *MRS Advan.* 6 (4) (2021) 125–130.
- [36] R. Middendorp, M. Dürr, A. Knott, F. Pointurier, D. Ferreira Sanchez, V. Samson, D. Grolimund, Characterization of the aerosol-based synthesis of uranium particles as a potential reference material for microanalytical methods, *Anal. Chem.* 89 (8) (2017) 4721–4728.
- [37] L.A. Rush, M.C. Endres, M. Liezers, J.D. Ward, G.C. Eiden, A.M. Duffin, Collisional dampening for improved quantification in single particle inductively coupled plasma mass spectrometry, *Talanta* 189 (2018) 268–273.
- [38] A. Gundlach-Graham, P.S. Garofalo, G. Schwarz, D. Redi, D. Günther, High-resolution, quantitative element imaging of an upper crust, low-angle cataclasis (Zuccale fault, Northern apennines) by laser ablation ICP time-of-flight mass spectrometry, *Geostand. Geoanal. Res.* 42 (4) (2018) 559–574.
- [39] A. Gundlach-Graham, S. Harycki, S.E. Szakas, T.L. Taylor, H. Karkee, R. L. Buckman, S. Mukta, R. Hu, W. Lee, Introducing “time-of-flight single particle investigator”(TOF-SPI): a tool for quantitative spICP-TOFMS data analysis, *J. Anal. Atomic Spectrom.* 39 (3) (2024) 704–711.
- [40] A.J. Goodman, H. Karkee, S. Huang, K. Pfaff, Y.D. Kuiper, Z. Chang, A. Gundlach-Graham, J.F. Ranville, Analysis of nano-mineral chemistry with single particle ICP-Time-of-Flight-MS; a novel approach to discriminate between geological environments, *Chem. Geol.* 671 (2025) 122498.
- [41] S.E. Szakas, R. Lancaster, R. Kaegi, A. Gundlach-Graham, Quantification and classification of engineered, incidental, and natural cerium-containing particles by spICP-TOFMS, *Environ. Sci. Nano* 9 (5) (2022) 1627–1638.
- [42] S. Harycki, A. Gundlach-Graham, Characterization of a high-sensitivity ICP-TOFMS instrument for microdroplet, nanoparticle, and microplastic analyses, *J. Anal. Atomic Spectrom.* 38 (1) (2023) 111–120.
- [43] H. Karkee, A. Gundlach-Graham, Characterization and quantification of natural and anthropogenic titanium-containing particles using single-particle ICP-TOFMS, *Environ. Sci. Technol.* 57 (37) (2023) 14058–14070.